

VIBROACOUSTIC ANALYSIS USING HYBRID FOURIER/3D MODELLING METHODS

P C Macey

PAFEC Limited, Strelley Hall, Nottingham, UK

1. INTRODUCTION

Vibroacoustic analysis is becoming a more commonly used tool for the underwater acoustics of submerged vehicles. This is due to the increase in computational power of available computers, the improvements in computational techniques and the emergence of commercial software using these methods. Axisymmetric problems can in general be treated very efficiently due to the reduced number of degrees of freedom required. Analysis of full 3D systems can be computationally expensive. Many systems are almost axisymmetric! The aim of the current work is to devise methods for efficiently analysing systems consisting of axisymmetric shells with 3D internal structure, immersed in an external fluid, eg fig 1 or fig 2.

Similar methods have been proposed before, ref [1]. The current work differs from ref [1] in the method of coupling between the 3D and Fourier meshes.

2. THEORY

It is proposed to use an axisymmetric (Fourier) model for the exterior shell and fluid and a 3D mesh for the internal parts.

Let the pressure in the surrounding fluid be expanded in a Fourier series as

$$p(r, \theta, x) = p_e(r, x) + \sum_{m=1}^{\infty} (p_m^e(r, x) \cos(m\theta) + p_m^o(r, x) \sin(m\theta)) \quad (1)$$

where the superfixes *e* and *o* are used to distinguish between even and odd harmonics.

Let $\{p_m^e\}$ and $\{p_m^o\}$ denote the nodal values of $p_m^e(r, x)$ and $p_m^o(r, x)$ respectively at the boundary element degrees of freedom.

FOURIER/3D MODELLING METHODS

The axial, radial and circumferential displacements on the shell can be similarly decomposed into a Fourier Series as:

$$\begin{aligned} U_o(r, \theta, x) &= U_{oo}^o(r, x) + \sum_{m=1}^{\infty} U_{om}^o(r, x) \cos(m\theta) + U_{om}^o(r, x) \sin(m\theta) \\ U_r(r, \theta, x) &= U_{ro}^e(r, x) + \sum_{m=1}^{\infty} U_{rm}^e(r, x) \cos(m\theta) + U_{rm}^o(r, x) \sin(m\theta) \\ U_c(r, \theta, x) &= U_{co}^o(r, x) + \sum_{m=1}^{\infty} U_{cm}^e(r, x) \sin(m\theta) - U_{cm}^o(r, x) \cos(m\theta) \end{aligned} \quad (2)$$

Let $\{U_m^e\}$ and $\{U_m^o\}$ denote the even and odd nodal displacements on the finite element mesh for the m th harmonic.

If the surrounding fluid can be assumed to be incompressible then the effect is simply an increase in the structure's inertia.

The discretised FE equations take the form:

$$([S_m] - \omega^2([M_m] + [E][M_f][E]^T))\{U_m^s\} = \{F_m^s\} \quad (3)$$

where S can be e or o , $[M_f]$ is the fluid virtual mass matrix and $[E]^T$ relates displacements on the structural mesh to normal displacements on the fluid mesh, see ref [2] for more details.

If the surrounding fluid is assumed to be compressible, then the coupled equations of the structural finite elements and acoustic boundary element are:

$$\begin{bmatrix} [S_m] + i\omega[C_m] - \omega^2[M_m] & [T_m]^T \\ -\omega^2\rho[G_m][E]^T & [H_m] \end{bmatrix} \begin{Bmatrix} \{U_m^s\} \\ \{p_m^s\} \end{Bmatrix} = \begin{Bmatrix} \{F_m^s\} \\ \{p_{lm}^s\} \end{Bmatrix} \quad (4)$$

as in ref [3]. The equations for the 3D internal structure are:

$$([S_{3D}] + i\omega[C_{3D}] - \omega^2[M_{3D}])\{U_{3D}\} = \{F_{3D}\} \quad (5)$$

When the two systems are coupled there will be additional forces on the right hand side of equations (3), (4) and (5) due to the other structure. The effect is that the harmonics become coupled via the internal 3D structure. The systems can be coupled by enforcing generalised constraints constructed from equation (2). These can be put in the form:

$$\{u_{3D}^b\} = [R]\{U_f\} \quad (6)$$

FOURIER/3D MODELLING METHODS

where $\{U_f\}$ denotes all the Fourier displacements and $\{U_{3D}^b\}$ are the 3D displacements on the interface with the Fourier mesh.

$$\{U_{3D}\} = \begin{Bmatrix} \{U_{3D}^b\} \\ \{U_{3D}^i\} \end{Bmatrix} \quad (7)$$

where $\{U_{3D}^i\}$ are the internal freedoms on the 3D mesh.

3. SOLUTION STRATEGY

There are two proposed solution strategies for solving equations (4) and (5). In the first scheme, the structural variables are eliminated initially. If a frontal solution is used then the constraint equations can be included in a straightforward manner. It is usually best for the element order to sweep as slowly as possible in the 'longest' direction of the structure. This requires only symmetric equations to be stored and solved during the structural elimination phase. However, the different harmonics become coupled and the solution for the acoustic surface pressures will require dividing by a complex asymmetric matrix of size NM by NM where N is the number of harmonics and M is the number of acoustic degrees of freedom per harmonic.

The second proposed solution strategy attempts a more efficient solution of the equations. Each harmonic is considered in turn. The boundary element freedoms for that harmonic are eliminated. Then any structural freedoms which do not occur in the constraints are eliminated. Finally a solution is performed solving for the displacement freedoms on the 3D elements and the Fourier displacement freedoms which occur in constraints. This method requires manipulation of complex asymmetric equations at all times. However it should be very efficient provided that relatively few Fourier freedoms are coupled to the 3D mesh. This would be true for the structure in figure 2, but not for that in figure 1.

If the evaluation of the acoustic boundary element matrices is significant in the overall computation time, then this could be reduced by using a generalisation of the methods of ref [4] and [5] for evaluating the Green's function.

4. TEST PROBLEM

The theoretical approach described in section 2, together with the first solution strategy described in section 3 has been implemented in the PAFEC VibroAcoustics program. A simple test problem has been devised. The structure is a cylindrical shell of radius 1m and length 4m with hemispherical endcaps and with an interior plate one quarter of the way along the length. The plate and shell have thickness 0.02m and material properties Young's modulus 209E9, Poisson's ratio 0.3 and density 7800kgm⁻³. The surrounding fluid is assumed to have density 1000kgm⁻³ and have an acoustic wavespeed of 1500ms⁻¹ for the compressible case.

The structure has been deliberately chosen to be axisymmetric, to permit comparison with pure Fourier modelling methods. To test the Fourier/3D coupling approach the external shell and fluid were modelled with Fourier elements and the internal plate was modelled with 3D shell elements.

FOURIER/3D MODELLING METHODS

The results computed are the natural frequencies for the structure vibrating in an incompressible fluid and the response of the system in a compressible fluid when excited by an incident plane wave of unit amplitude approaching at an angle of 45° to the axis, see figure 3.

5. COMPUTATIONAL MODELS AND RESULTS

The Fourier model used to analyse the structure is shown in figure 4. It consists of 22 3-noded shells of revolution using the formulation of reference [6]. The boundary element consisted of 16 3-noded line patches. For the 3D internal structure the 6 elements used to model the plate were replaced by a mesh of 144 6-noded semi-Loof triangles as in figure 5. Some analyses were also performed using the fully 3D model shown in figure 6 consisting of 168 6-noded triangle and 168 8-noded quadrilateral semi-Loof elements.

Table 1 shows a comparison of natural frequencies for the Fourier/3D models, taking harmonics 0,1,2 and the Fourier model for the structure in vacuo. Table 2 shows the natural frequencies in incompressible fluid.

Table 1 Natural frequencies in vacuo

Frequency No. (Fourier/3D)	Frequency (Fourier/3D)	Frequency (Fourier)	Harmonic
7	49.44	49.45	0
8	100.6	100.9	1
9	100.6	100.9	1
10	130.2	130.1	2
11	130.2	130.1	2
12	164.2	165.5	2
13	164.6	165.5	2

Table 2 Natural frequencies in fluid

Frequency No. (Fourier/3D)	Frequency (Fourier/3D)	Frequency (Fourier)	Harmonic
7	49.13	49.13	0
8	71.77	71.76	2
9	71.77	71.76	2
10	100.5	100.8	1
11	100.5	100.8	1
12	164.1	165.4	2
13	164.5	165.4	2

Figure 7 shows results for the axial displacement against frequency at the centre of the internal plate for the excitation by incident plane wave in a compressible fluid. Comparison is made between the Fourier/3D approach using harmonics 0,1,2,3,4 and the full 3D model. The discrepancy in resonant frequencies is thought to be due to a difference in shell theories between the semi-loof elements and the Fourier shell elements of ref [6]. This matter is being investigated.

FOURIER/3D MODELLING METHODS

The results computed by the Fourier/3D model required considerably less computation time. It is expected that the new method will be faster still when the second solution strategy has been implemented.

6. CONCLUSIONS

The proposed Fourier/3D modelling method has been shown to work. It offers considerable promise of being a very efficient technique for solving vibroacoustic problems for submerged axisymmetric shell systems containing internal 3D structure.

7. REFERENCES

- [1] M H Ettouney, R P Daddazio and N N Abboud
"The interaction of a submerged axisymmetric shell and three dimensional internal systems"
Int. Jou. Num. Meth. Eng. Vol 37 1994 pp2951-2970
- [2] P C Macey
"Acoustic and structure interaction problems using finite and boundary elements"
PhD Thesis, Nottingham University 1987
- [3] P C Macey
"Oblique incidence diffraction by axisymmetric structures"
Proc. IOA. Vol 16 pt 6 1994 pp 67-74
- [4] T W Dawson
"On integral representations for the axially symmetric Helmholtz Green's function"
Appl. Math. Modelling Vol 19 pt 10 1995 pp583-589
- [5] T W Dawson
"On the singularity of the axially symmetric Helmholtz Green's function with application to BEM"
Appl. Math Modelling Vol 19 pt 10 1995 pp 590-600
- [6] J J Webster
"Free vibrations of shells of revolution using finite elements"
Int. Jou. Mech. Sci. Vol 9 1967 pp 559-570

FOURIER/3D MODELLING METHODS

Figure 1

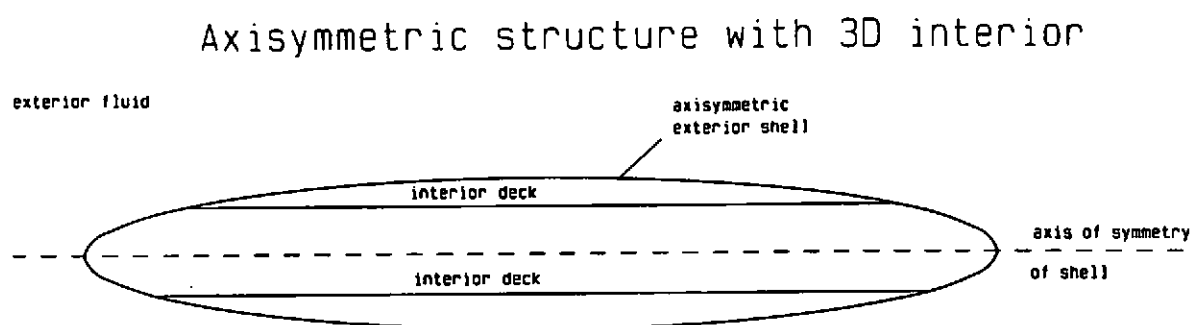
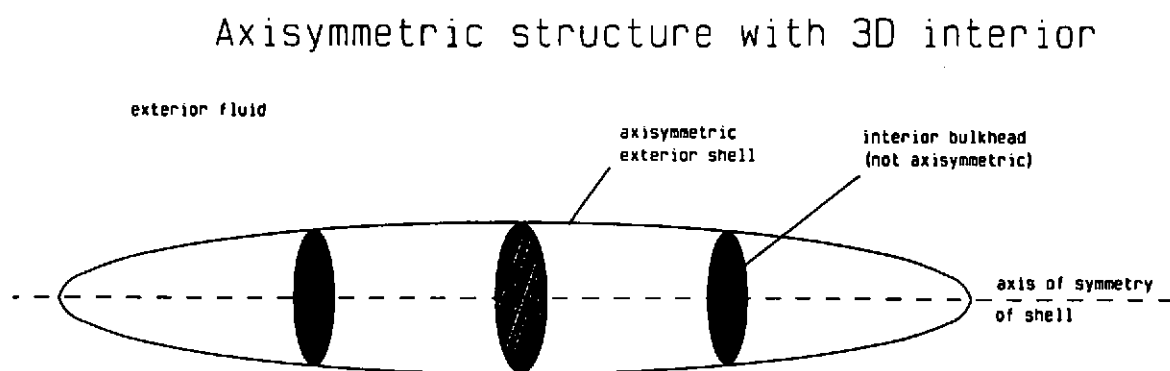


Figure 2



FOURIER/3D MODELLING METHODS

Figure 3

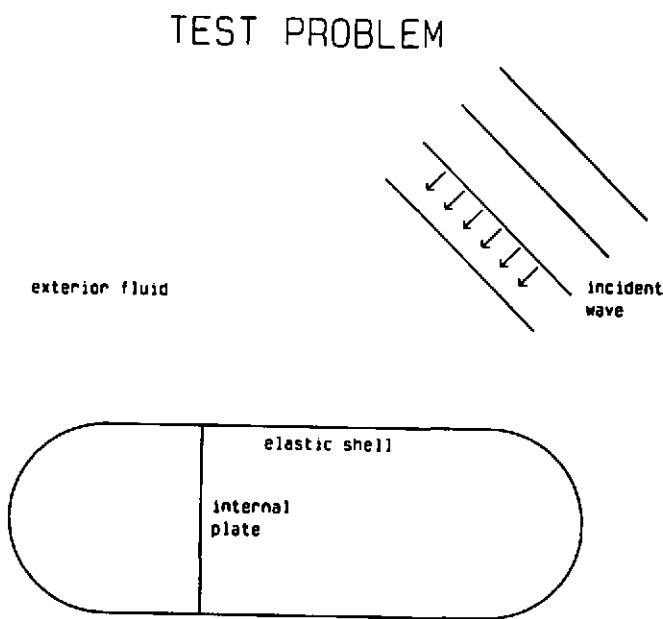
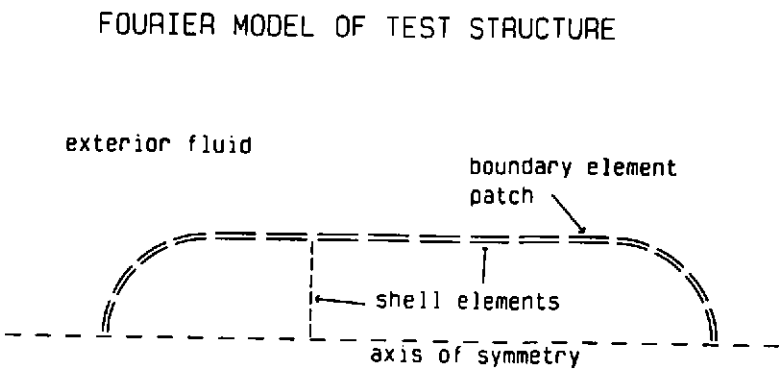


Figure 4



FOURIER/3D MODELLING METHODS

Figure 5

3D MODEL OF INTERNAL PLATE

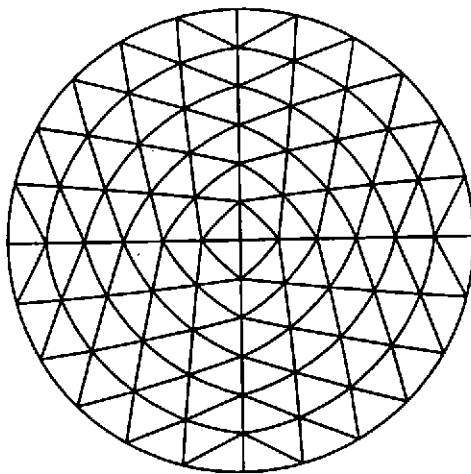
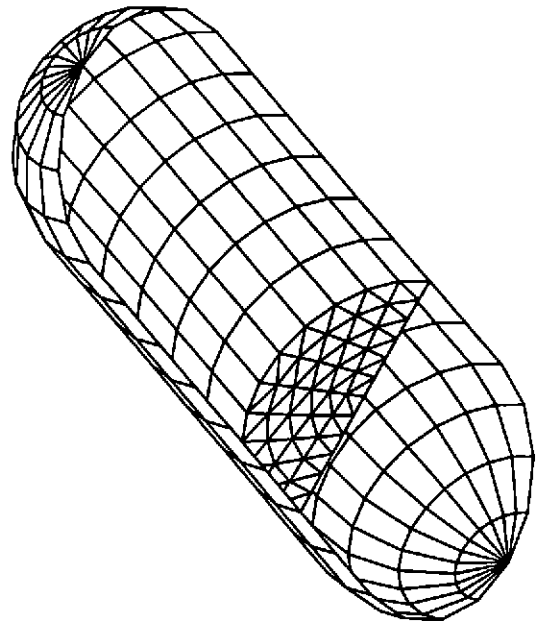


Figure 6

3D model of test structure



DISPLACEMENT AT CENTRE OF INNER PLATE
EXCITATION BY INCIDENT PLANE WAVE

Figure 7

